Available online at www.sciencedirect.com
ScienceDirect
Solid-State Electronics 52 (2008) 211–214
SOLID-STATE ELECTRONICS
www.elsevier.com/locate/sse

High-efficiency red phosphorescent organic light-emitting diodes based on metal-microcavity structure

X.Y. Sun [a,b], W.L. Li [a,*], M.L. Xu [c], B. Chu [a], D.F. Bi [a], B. Li [a], Y.W. Hu [b], Z.Q. Zhang [d], Z.Z. Hu [d]

[a] *The Key Laboratory of Excited State Processes, Changchun Institute of Optics, Fine Mechanics and Physics, Chinese Academy of Sciences, 16-Dong Nan Hu Road, Economic Development Area, Changchun 130033, PR China*
[b] *College of Mechanical and Electronics, Central South University, Changsha 410083, PR China*
[c] *Xi'an Modern Chemistry Research Institute, Xi'an 710065, PR China*
[d] *The Organic Photoelectronic Material Research and Development Center, Anshan University of Science and Technology, Anshan 110044, PR China*

Received 7 November 2006; received in revised form 3 September 2007; accepted 5 September 2007
Available online 15 October 2007

The review of this paper was arranged by Prof. Y. Arakawa

Abstract

Multilayer electroluminescent (EL) diodes with red emission were fabricated using Bis(2-(2′-benzo[4,5-α]thienyl)pyridinato-N,$C^{3'}$) iridium (acetyl-acetonate) [$(btp)_2Ir(acac)$] as dopant. Double metal-microcavity structure with a semitransparent Ag anode was introduced into the EL diodes. The cavity device structure was ITO/Ag/*N*,*N*′-di(naphthalene-1-yl)-*N*,*N*′-diphenyl-benzidine [NPB]/4,4′-*N*,*N*′-dicarbazole-biphenyl [CBP]: 5 wt% $(btp)_2Ir(acac)$/2,2′,2″-(1,3,5-benzenetriyl)tris[1-phenyl-1*H*-benzimidazole] [TPBi]/LiF/Al. The sharp bright red emission of cavity device was observed. Compared with noncavity device the full width at half maximum (FWHM) of top normal emission spectrum was narrowed from 38 nm to 23 nm, and the maximum brightness of the cavity device was increased from 3500 cd/m^2 to 5800 cd/m^2, i.e., was improved by a factor of 1.7. The blue-shift of emission spectrum with increasing detection angle in traditional microcavity device was no longer observed, which attributed to a very steep rising of the EL-emission from $(btp)_2Ir(acac)$. Besides, it was importantly found that at higher current density EL efficiency was obviously higher for the cavity device than for noncavity device, i.e., at $J = 200$ mA/cm^2 the former and later were 1.8 cd/A and 1.0 cd/A, respectively. And the increasing mechanism of the EL efficiency was ascribed to the shortened lifetime of triplet excited state (T_1) and the weakened hole injection of Ag anode.

PACS: 85.30.−z; 85.60.Jb

Keywords: OLEDs; Phosphorecent; Microcavity; Lifetime

1. Introduction

Organic light-emitting devices (OLEDs) are one of the best current candidates to meet the critical properties, including mechanical robustness, reliability, full color, light weight, and high efficiency. Over the last two decades, advances in OLED efficiencies have been made through the synthesis of efficient lumophores, optimization of the OLED structure, and doping technology of OLEDs with highly emissive phosphorescent and fluorescent materials [1–3]. The process of charge injection and recombination in OLEDs results in the generation of either excited-singlet state or -triplet state. According to quantum statistics, the singlets excitons of direct generation are limited to 25%, while the rest of the excitons, 75%, are triplets. For the electro-fluorescent OLEDs, only the singlet excitons contribute to the light generation processes [4], which provide the

* Corresponding author.
E-mail address: wllioel@yahoo.com.cn (W.L. Li).

0038-1101/$ - see front matter © 2007 Elsevier Ltd. All rights reserved.
doi:10.1016/j.sse.2007.09.001

external quantum efficiency up to 5% [5]. By using phosphorescent dyes in an appropriate host material [6,7], because of the contribution of both singlet- and triplet-excitons to the EL-emission, quantum efficiency is increased significantly.

Generally, the EL lifetime of phosphorescent device is much longer than that of fluorescent device [7–9], which could induce T–T annihilation and saturation of the ligand-excited state. Therefore, at higher current density, the EL efficiencies of the devices based on phosphorescence emitting materials would drop obviously. Because the efficiencies were approximately proportional to the lifetime of the excited state [8], and the performances of the phosphorescent device were more sensitive to the properties of surrounding media compared to devices based on fluorescent emitters. So minimizing annihilation and saturation of the ligand-excited state [7,9] and decreasing the probability for non-radiative decay [6] are the key issues for increasing efficiency at higher current density. Besides, the relative longer radiative lifetime of phosphorescent materials is a crucial factor for the population reversion of achievement in organic laser diodes (OLDs). Therefore, researchers are interested in enhancing the EL efficiency by optimizing the device structure based on phosphorescent materials, such as, introducing semitransparent Ag as anode, which was reported in Refs. [10,11]. And the phosphorescent devices based on semitransparent Ag anode were fabricated, which exhibited a maximum current efficiency of 81 cd/A and a power efficiency of 79 lm/W. However, their EL efficiency at high current density dropped drastically. In order to resolve the current-saturation problem of the electro-phosphorescent devices, we designed the devices with double metal mirror Fabry-pérot microcavity. Since microcavity structure can shorten the lifetime of the excited state, it can improve the EL efficiency at high current density.

2. Experimental

The Ir-complex was synthesized in our laboratory. Microcavity OLEDs and control devices were grown onto the pre-cleaned 100 Ω/□ glass substrates in the same vacuum by high vacuum ($<5.0\times10^{-4}$ Pa) thermal evaporation. The cavity device comprised of a 33-nm-thickness semitransparent Ag mirror with the reflectance of ~80%, 55-nm-thickness NPB [*N*,*N*′-di(naphthalene-1-yl)-*N*,*N*′-diphenyl-benzidine] as the hole transporting layer (HTL), a 20-nm-thickness 4,4′-*N*,*N*′-dicarbazole-biphenyl [CBP]: 5 wt% Bis(2-(2′-benzo[4,5-α]thienyl) pyridinato-N,C3′) iridium (acetyl-acetonate) [$(btp)_2Ir(acac)$] as the emitting layer (EML), a 55-nm-thickness 2,2′,2″-(1,3,5-benzenetriyl)tris[1-phenyl-1*H*-benzimidazole] [TPBI] as the electron transporting layer (ETL), and a cathode comprised of 0.5-nm LiF and 100-nm-thickness Al, the device configurations are shown in Fig. 1a. The comparable device (shown in Fig. 1b) possesses of the same organic layers and cathode. The EL spectra were detected by Hitachi F-4500 fluorescent spectra meter. The luminance–voltage characteristics were measured simultaneously by a DC power supply combined with a spot photometer. The photoluminescence (PL) decay times were measured by a spectrometer, a photomultiplier, a boxcar averager and the sample was excited by YAG:Nd laser at a wavelength of $\lambda = 355$ nm. The active area of the devices was 2×2 mm^2. All the tests were carried out in the ambient.

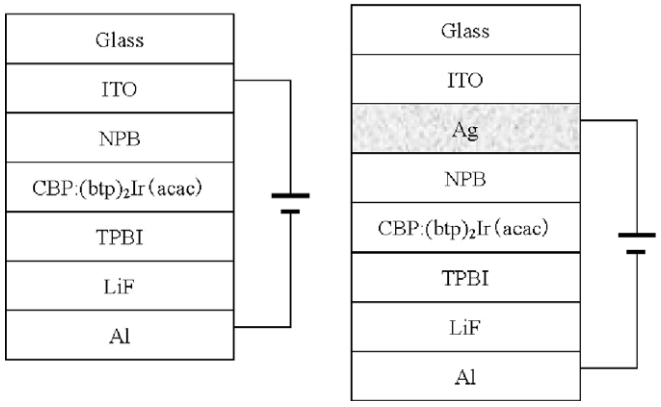

Fig. 1. The structures of cavity: (a) and noncavity (b) EL devices based on $(btp)_2Ir(acac)$.

3. Results and discussion

The top normal EL spectra of control device and cavity operated at 10 V are shown in Fig. 2 (seen the curve 1 and 2, respectively). It can be seen that compared with noncavity device the full width at half maximum (FWHM) of top normal emission spectrum of cavity device was narrowed from 38 nm to 23 nm. Another EL band centered at 670 nm was depressed drastically in cavity device, because of the resonant peak of cavity device was designed centering at 620 nm, that is, only the emission around 620 nm could be enhanced, other mode of emission was depressed. Although the EL color purity was affected a little, the color saturation purity approaching to the emission of Eu^{3+} complex [12]. The 30° and 60°-off normal emission spectra in the cavity device were also shown in Fig. 2 (curve-3 and -4, respectively). It can be seen that the EL-emission cen-

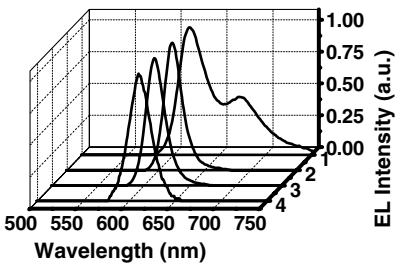

Fig. 2. EL spectra of cavity and noncavity devices detected at 10 V. Spectra 1 and 2 represent the noncavity and top normal emission of cavity devices, respectively; spectra 3 and 4 represent the 30° and 60°-off top normal emission of cavity devices, respectively.

tered at 617 nm is not changed with the detecting angle obviously, which should be ascribed to two reasons, one is the spontaneous emission matched with the resonant peak, the other is the steep rise of emission spectra of phosphorescent Ir-complex compared with other wide band emission materials. The Commission International de I'Eclairage (CIE) coordinates corresponding to the detecting angles were not varied obviously. At normal emission, for cavity and noncavity devices, they were ($x = 0.664$, $y = 0.336$) and ($x = 0.656$, $y = 0.344$), respectively, which were closing to the National Television Standards Committee recommended red primary color for a video display, and were much better than those of based on DCM doping devices [12,13]. Thus, the microcavity devices based on $(btp)_2Ir(acac)$ overcame the defect of traditional cavity devices, i.e., the blue-shifting of emission peaks with the increasing of detection angle was weakened [9,12].

Fig. 3 shows the dependence of current efficiency on driving current density for the cavity and noncavity devices, it can be seen that the maximum current efficiency of 4.6 cd/A and 3.3 cd/A was obtained at $J = 20$ mA/cm^2 in cavity device and at $J = 0.2$ mA/cm^2 in control device, respectively. At lower current density, the efficiency is lower in cavity device, which due to the worse carrier injection of the un-treatment Ag anode [14]. However, a remarkable improvement of current efficiency at high current density can be observed in cavity device, that is, at $J = 200$ mA/cm^2 the cavity device shows higher efficiency compared with noncavity device (1.8 cd/A versus 1.0 cd/A). And the characteristic current (J_0) at which current efficiency fallen to 50% of its peak value due to the triplet–triplet (T–T) annihilation was 200 mA/cm^2 in cavity device, even considering the fall of the same current efficiency (from 3.3 cd/A dropped to 1.7 cd/A), in noncavity device J_0 was 19 mA/cm^2. The current-saturation phenomenon was considerably improved at higher driving current density. The microcavity determines the electric-field mode distribution, thereby modifying the exciton spontaneous emission lifetime [15]. According to the PL lifetime of

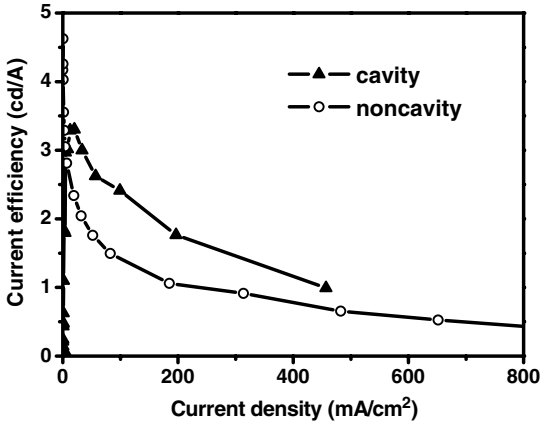

Fig. 3. Dependence of the EL efficiency of cavity (▲) and noncavity (○) devices on the current density.

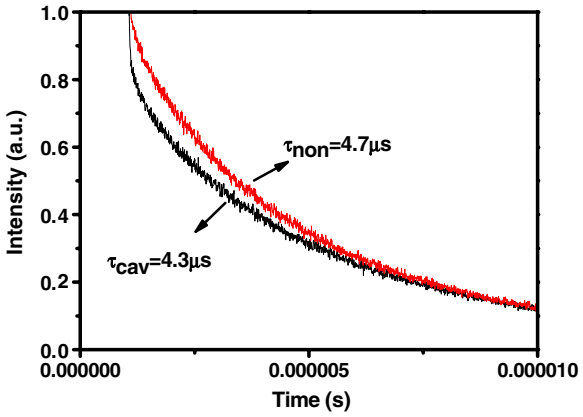

Fig. 4. The PL lifetime of (btp)2Ir(acac) mono-films and that in cavity device.

$(btp)_2Ir(acac)$ films, as was shown in Fig. 4, it was shortened from 4.7 μs (neat film) to 4.3 μs (film sandwiched in the double metal mirrors). Since for phosphorescent devices, each T–T annihilation event generates a single triplet-exciton, the concentration of triplet-excitons, $[^3M^*]$, is determined by the rate of triplet generation (proportional to current density), the total T–T annihilation rate is $k_{TT}[^3M^*]$, and assuming that the luminescence intensity (L) is linearly proportional to the concentration of excited states, i.e., then the phosphorescent emission intensity is [16]

$$L(t) = \frac{L(0)}{(1 + K\tau)e^{t/\tau} - K\tau}, \tag{1}$$

where K is defined by

$$K = \frac{1}{2}k_{TT}[^3M^*(0)]. \tag{2}$$

The quantum efficiency of light emission (η) can also be given

$$\frac{\eta}{\eta_0} = \frac{J_0}{4J}\left(\sqrt{1 + 8\frac{J}{J_0}} - 1\right), \tag{3}$$

where η_0 is the quantum efficiency in the absence of T–T annihilation and J_0 is proportional to τ^2, the roll off of current efficiency with J is consistent with the lifetime (τ) [7]. On the other hand, comparing with control device, the worse carrier injection of un-treatment Ag anode can depress hole injection of cavity device, as was shown in the dependence of current density on driving voltage in Fig. 5, which is propitious to the balance of carriers. Therefore, the improvement of efficiency (η_{ext}) in cavity device at high driving current density was due to the shortened lifetime which resulted from electric-field mode redistribution caused by the cavity structure [17] and the balance of carriers [18].

Fig. 5 shows the dependence of luminance on driving voltage at the same time, it can be observed that the peak luminance of 5840 cd/m^2 was obtained at 21 V in the cavity device, which is larger than that (3460 cd/m^2 at 14 V) of

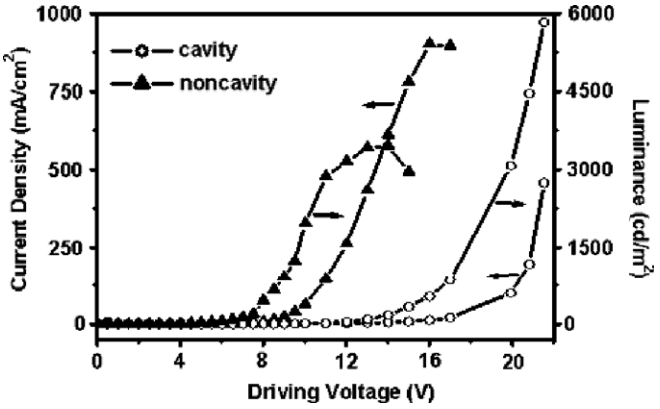

Fig. 5. Dependence of the current density and luminance of cavity (▲) and noncavity (○) devices on the operating voltage.

noncavity device by 1.7 times. The enhancement of light output should be attributed to the resonant effect of the cavity structure [9]. However because of the worse carrier injection of the un-treatment Ag anode, the turn on voltage in cavity device (8.5 V) was higher than that in noncavity device (3.5 V), which can be approved by CF_4 plasma pre-treatment of the Ag anode [10].

4. Conclusion

In summary, phosphorescent OLEDs with microcavity structure was constructed, which can demonstrate bright pure red emission. The phenomenon of emission peak blue-shifting with the increasing of detection angle was not evident. Because of the narrowed emission peak, better color purity was achieved. A more important finding is that a significant improvement in current efficiency at high current density compared with noncavity device, which should due to the shortened lifetime of the excited state caused by the coupled effect of exciton and photon, thereby minimizing the T–T annihilation. The improvements of EL efficiency at higher current and color purity of cavity OLEDs are favor of the potential application of microcavity structure devices in full color displays and organic electrical lasers (OEL).

Acknowledgements

This work is founded in part by the National Science Research Project (No. 90201012) of China. The authors are deeply grateful to S.Z. Lv for the measurement of PL lifetimes.

References

[1] Tang CW, Van Slyke SA. Appl Phys Lett 1987;51:913.
[2] Baldo MA, O'Brien DF, You Y, Shoustikov A, Sibley S, Thompson ME, et al. Nature (London) 1998;395:151.
[3] Baldo MA, Lamansky S, Burrows PE, Thompson ME, Forrest SR. Appl Phys Lett 1999;75:4.
[4] Adachi C, Baldo MA, Thompson ME, Forrest SR. J Appl Phys 2001;90:5048.
[5] Greenham NC, Friend RH, Bradley DDC. Adv Mater 1994;6:491.
[6] Adachi C, Baldo MA, Forrest SR, Thompson ME. Appl Phys Lett 2000;77:904.
[7] Adachi C, Baldo MA, Forrest SR. J Appl Phys 2000;87:8049.
[8] Klessinger M, Michl J. Excited states and photochemistry of organic molecules. New York: VCH; 1995.
[9] Jordan RH, Rothberg LJ, Dodabalapur A, Slusher RE. Appl Phys Lett 1996;69:1997.
[10] Peng HJ, Sun JX, Zhu XL, Yu XM, Wong M, Kwoka HS. Appl Phys Lett 2006;88:073517.
[11] Peng HJ, Zhu XL, Sun JX, Yu XM, Wong M, Kwok HS. Appl Phys Lett 2006;88:033509.
[12] Adachi C, Baldo MA, Forrest SR, Lamansky S, Thompson ME, Kwong RC. Appl Phys Lett 2001;78:1622.
[13] Sun XY, Li WL, Hong ZR, Wei HZ, Zang FX, Chen LL, et al. J Appl Phys 2005;97:103112.
[14] Chen CW, Hsien PY, Chiang HH, Lin CL, Wu HM, Wu CC. Appl Phys Lett 2003;83:5127.
[15] Pellegrini V, Tredicucci A. Phys Rev B 1995;52:R14328.
[16] Baldo MA, Adachi C, Forrest SR. Phys Rev B 2000;62:10967.
[17] Lidzey DG, Bradley DDC, Skolnick MS, Virgili T, Walker S, Whittaker DM. Nature 1998;395:53.
[18] Wang ZJ, Wu Y, Zhou YC, Zhou J, Zhang ST, Ding XM, et al. Appl Phys Lett 2006;88:222112.